Volume 66, Issue 5, 2022
Journal of Scientific Research
of
The Banaras Hindu University

A statistical analysis of X- class solar flares and their association with the super active regions during solar cycles 23- 24

Abha Singh[1], Anurag Chaudhary[1], V. S. Rathore[2] and A. K. Singh[2*]

[1]Department of Physics, T D P G College, Jaunpur-222002, U.P. India
[2]Atmospheric Research Laboratory, Department of Physics, Banaras Hindu University, Varanasi-221005, UP, India.
[*]singhak@bhu.ac.in

Abstract: **The A statistical distribution function of X-class flares and their association with super-active regions (SARs) during two recent solar cycles 23-24 have been analyzed. The obtained results show that, during solar cycle 23, 57.60 % of the total number of X-class flares coincides with a set of X1.0 - X1.9 flares, 15.20 % to X2.0 - X2.9, 12.80 % to X3.0 - X4.9, 9.60 % to X5.0 - X9.9, and 4.80 % to ≥ X10 flares. During solar cycle 24, 61.20 % of the total number of X-class flares coincides with a set of X1.0 - X1.9 flares, 22.40 % to X2.0 - X2.9, 8.16 % to both the X3.0 - X4.9 flares, and X5.0 - X9.9 flares. None of the ≥ X10 flares. All X-class flares are found to be in a scattered manner in solar cycles 23 and 24. Among the cycles, solar cycle 24 has been observed relatively very weak cycle and the total number of X-class flares diminished in comparison to previous solar cycles. During solar cycle 23, 29.16% of the X1.0 - X1.9 flares, 36.84 % of the X2.0 - X2.9 flares, 43.75 % of the X3.0 - X4.9 flares, 83.33 % of both the X5.0 - X9.9 flares, and 100.00 % of the ≥ X10 flares were produced by SARs. While during solar cycle 24, 20.00 % of the X1.0 - X1.9 flares, 36.36 % of the X2.0 - X2.9 flares, 25.00 % of the X3.0 - X4.9 flares, 75.00 % of the X5.0 - X9.9 flares, and 0.00 % of the ≥ X10 flares were produced by SARs.**

Index Terms: **Solar flare; Solar Cycle, Super active region.**

I. INTRODUCTION

This document The limited regions (areas) of intense and complex magnetic fields on the Sun that traveled across the Sun's Earth-facing side with normal rotation are termed active regions (ARs) (Yang et al. 2017). ARs are the primary cause of all solar activity such as sunspots, flares, coronal mass ejections, gradual and impulsive enhancements of radiation in the extreme ultra-violet (EUV), X-ray, and radio region of the solar spectrum, and acceleration of fast electrons and protons (Bruzek 1972). The types of different solar activities and their intensity dependence on the evolutionary track of an AR are found to be strongest at the appearance stage and then fade up slowly after that critical stage. The number of sunspots is one of the most decisive and critical parameters to ascertain the occurring active solar phenomena (van Driel-Gesztelyi and Green 2015). The number of sunspots observed on the visible solar disk is the measure of the strength of solar activity, which is also found to be cyclic in nature. This cycle exhibits a time period of ~ 11 years on average and is referred to as the solar cycle (Schwabe and Schwabe 1844). A solar cycle has many active regions, but only a few ARs would produce remarkably strong solar flares (Wang and Liu 2015).

Solar flare activity is directly associated with sunspots, unequal brightening of the Sun's surface. Depending on the wavelength of emitted X-rays (ranges 1-8 Å), Solar flare usually may be categorized into classes X, M, C, or B (Carrington 1859). The flux peak of these class flares X, M, C, or B is of order 10^{-4}, 10^{-5}, 10^{-6}, and 10^{-7} watts m^{-2} respectively, measured by the geostationary operational environment satellite (GOES) since 1996. Sammis et al. (2000) have observed that the solar active regions, having the largest and most complex sunspot groups, are found to be suitable for the observation of relatively stronger solar flares. A Super Active region is defined as one which can produce exceptionally strong flares. Bai (1987) was the first one to introduce the concept of the active region. Then several researchers studied SARs and given various definitions (Bai 1988; Chen et al. 2011; Li and Wang 1997; Romano and Zuccarello 2007; Roy 1977; Tian et al. 2002; Wu and Zhang 1995).

Recently, Isaeva et al. (2020) reported that 78.00% of the solar flares are produced during solar cycle 24 occur predominantly in activity complex (ACs) groups of sunspots based on a relationship between intense solar flares (> M1.0) and activity complex on the Sun.Bruevich et al. (2017) also analyzed the large

(X-ray class > M1.0) and very large (X-ray class > X1) flares that remain present in solar activity cycle 24 and conclude the flare activity in cycle 24 was significantly weaker than in cycles 21–23, according to the observational inputs (GOES-15, M1 – X7 class) and SDO/EVE (EUV – range). Mohamed et al. (2018) reported after analyzing the ARs for the solar cycles 23 and 24 that the high energetic solar flares (X-class flares) become more prominent during the maximum solar activity period and produces at other phases of solar activity, with special emphasis on the declining phases.

A definition of SAR was proposed by Chen et al. (2011) considering the parameters such as the maximum area of sunspot groups, soft X-ray flare index, peak flux of 10.7 cm, and short-term solar irradiations decrease (<0.01). Harra et al. (2016) reported that the observed powerful and intense solar flares do not correspond to large sunspot areas. Le et al. (2014) employed these active regions to study X-ray flares' statistical properties and their correlation with active regions during solar cycles 21-23. Despite various above-reported studies, the complete statistical correlation between super active regions and intense solar flares is least understood and under-explored. To minimize this gap in the literature and to find a better relationship and understate, the present study has been initiated using the two recent solar cycles.

In this paper, a statistical analysis of intense X-class solar flares and their relationship with SARs observed during the two recent solar cycles 23-24 are explored. During the solar cycle, 23-24, a total number of 39392 C-class weak solar flares, 3295 M-class moderate solar flares, and 174 X-class intense flares were observed. These 174 X-class intense solar flares were associated with a total of 88 active regions. Out of these 88 active regions, only 17 are selected as SARs according to the criteria of a super active region given in Chen and Wang (2015) and Chen et al. (2011). The X-class solar flares are further categorized according to their intensities. The method of data selection in the present study is presented in section 2 and the results and discussions are presented in section 3. Finally, the conclusions of the present study are presented in section 4.

II. Method of Data Selection

The 13-month smoothed monthly sunspot numbers (SMSNs) are used to describe the progress of a solar cycle. The SMSNs profile can be collected from the website http://www.sidc.be/silso/datafiles#total. The period from the minima to the maxima of SMSNs is presented as the ascending phase and that from one month after the maximum of SMSNs to the minimum of SMSNs is known as a descending phase of the solar cycle. The maxima of SMSNs are defined as the solar cycle size or the solar cycle intensity (Le et al. 2014). The maximum SMSNs of solar cycle 23 is 180.3, observed in November 2001, and 116.4 of solar cycle 24 observed in April 2014.

The X-ray solar fluxes on their peak emission in the 0.1 – 0.8 nm are simply monitored by Geostationary Orbital Environmental Satellite (GOES-15) under the NOAA/NASA. The flares mentioned in this paper can be obtained from the website https://www.spaceweatherlive.com/en/archive. For each SARs observed during the 23 and 24 solar cycles, flare index has been calculated, and the relative **β-γ-δ** magnetic field of sunspot group days is also taken into account to show the high magnetic field. The start date and end date of SARs have been included also.

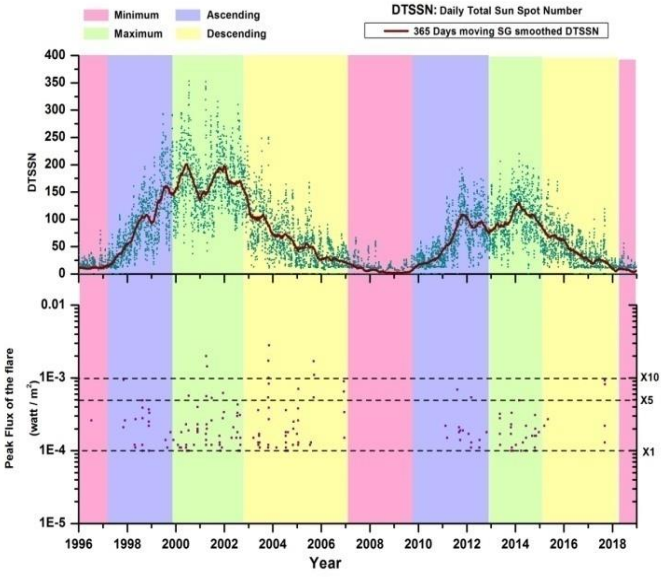

Fig. 1: The distributions of X-class flares during 23-24 cycles.

III. Results and Discussion

A. *The Statistical distribution of X-class flares*

There Total 174 X-class flares and 88 ARs occurred during solar cycle 23-24 are analyzed. 125 flares belong to solar cycle 23, and 49 flares occurred in solar cycle 24. It is observed that 102 flares (58.62%) with the range X1.0 - X1.9 out of 174 flares, 30 flares (17.24 %) at X2.0 - X2. 9,20 flares (11.49 %) at X3.0 - X4.9 level, 16 flares (9.19 %) at X5.0 - X9.9, 6 (3.44 %) at ≥ X10. It is also noticed, there are no ≥ X10 flares in solar cycle 24. The distributions of X-class flares during solar cycles23-24 are presented in Figure 1. The maximum of SMSNs is 180.3 for solar cycles 23 and 116.4 for solar cycles 24. From the graph, it is clear that more than 50.00 % of flares of different intensities occurred in the descending phase of the solar cycle 23, while the appearance of X-flares in the observed pattern is more in the ascending phase of the solar cycle 24 except (X2.0 - X2.9) intensity.

Table 1 represents the distribution of all X class flares of different intensities that occurred in the solar cycle 23. From table 1, it is evident that 57.60 % of the X1.0 - X1.9 flares, 15.20 % of the X2.0 - X2.9 flares, and 12.80 % of the X3.0 - X4.9 flares, 53.27 % of the X1.0 - X4.9 flares, 9.60 % of the X5.0 - X9.9 flares, and 4.80 % of the ≥ X10 flares occurred during solar cycle 23. Further, it is also noted that 45.83 % and 54.16 % of the total X1.0 - X1.9 flares, 63.15 % and 36.84 % of the total X2.0 - X1.9

flares, 31.25 % and 68.75 % of the total X3.0 - X4.9 flares, 46.72 % and 53.27 % of the total X1.0 - X4.9 flares and 33.33 % and 66.67 % of the total ≥X5 flares appeared in ascending and descending phases of this solar cycle respectively. On average of all flares intensity, 44.80 % and 55.20 % of the solar flares occurred in ascending and descending phases of this solar cycle respectively. It is also observed that 44.00 % and 72.20 % of the X1.0 - X1.9, 42.00 % and 58.00 % of the X2.0 - X2.9 flares, 50.00 % and 56.25 % of the X3.0 - X4.9 flares, 45.00 % and 67.20 % of the X1.0 - X4.9 flares, and 55.50 % and 61.10 % of the ≥ X5.0 flares appeared one year before and two years after (N_{12}) and two years before and three years after (N_{23}) these solar cycle maxima respectively.

Table 2 represents the distribution of all X-class flares of different intensities that occurred in solar cycle 24 and it is observed that on average of all flares intensity, mostly X-flares (63.20 %) occurred in the ascending phase of the cycle with the pattern of flares intensity, 70.00 % of X1.0 - X1.9, 45.50 % of X2.0 - X2.9, 75.00 % of X3.0 - X4.9, 64.44 % of the X1.0 - X4.9 flares and 50.00 % of ≥ X5.0 and 36.70 % flares in the descending phase of this solar cycle with the pattern of flares intensity, 30.00 % of X1.0 - X1.9, 54.54 % of X2.0 - X2.9, 25.00 % of X3.0 - X4.9, 35.55 % of the X1.0 - X4.9 flares and 50.00 % of ≥ X5.0 flares.

Corresponding to the maxima of solar cycle 24, 70 % of the X1.0 - X1.9 flares appeared in the N_{21} range (two years before and one year after the peak) and 93.00 % of them occurred in the N_{32} range (three years before and two years after the peak). Also, 63.60 % and 72.20 % of the X2.0 - X2.9 flares appeared in N_{21} and N_{32} range respectively. 100.00 % of the X3.0 - X4.9 flares appeared in both the N_{21} and N_{32} range. 71.10 % and 88.80 % of the X1.0 - X4.9 flares appeared two years before and one year after (N_{21}) and three years before and two years after (N_{32}) of this solar cycle maxima, respectively. It is also found that there is no ≥ X5 flare that appeared two years before and one year after (N_{21}) the solar cycle maxima, but 50.00 % of this level flares appeared three years before and two years after (N_{32}) of this solar cycle maxima. It is also noticed that no ≥X10 flare occurred in solar cycle 24 that means this solar cycle is weaker than their preceding solar cycles.

B. Association of solar flares with Super Active Regions (SARs)

There were 174 X-class flares produced by 88 active regions. Out of 88 ARs, 59 ARs were associated with 125 solar flares that occurred in solar cycle 23, while 29 ARs were associated with 49 solar flares that occurred in solar cycle 24. Out of 88 ARs, only 17 active regions, are selected as super active regions according to criteria for the definition of SARs is given by Chen et al. (2011) such as the maximum area of the sunspot group, the solar flare index (of M and X class-class flare), the maximum 10.7 cm radio flux. Along with these criteria we have considered ARs as super active regions which produced a large number of solar flares (of M and X Class) in which at least one X –class flare was involved. Out of 17, 70.60 % (12) of SARs belong to solar cycle 23, and 29.41 % (5) belong to solar cycle 24. The properties of these SARs, which produced highly energetic X-class flares, when they cross the solar disk, are given in Table 4. For each SARs start and end dates, maximum sunspots numbers, the maximum area of the sunspot group, the solar flare index, the maximum 10.7 cm radio flux, the maximum days of beta-gamma-delta (β-γ-δ) class of sunspot group, total numbers of X-class flares produced from that region and its location in the northern or southern hemisphere are shown in this table. Beta-Gamma-Delta (β-γ-δ) magnetic field is considered to be the strongest of all magnetic field types of sunspots. Mohamed et al. (2018) reported that there is coherence between the number of X-flares and the number of days of (β-γ-δ) magnetic field during the solar cycle 23-24.

Table 3 shows that during the solar cycle 23, out of 59 active regions, 12 are SARs (20.00 %) and (80.00 %) are ARs. These 12 SARs produced 29.16 % of the X1.0 - X1.9 flares, 36.84 % of the X2.0 - X2.9, 43.75 % of the X3.0 - X4.9 flares, 83.33 % of the X5.0 - X5.9 flares, and 100.00 % of the ≥X10 flares. Whereas in solar cycle 24, 17.24 % of (5 ARs) the total ARs (29) is considered as super active regions (SARs), which produced 20.00 % of the X1.0 - X1.9 flares, 36.40 % of the X2.0 - X2.9, 25.00 % of the X3.0 - X4.9 flares, and 75.00 % of the X5.0 - X5.9 flares. There were no ≥ X10 level flares in solar cycle 24.

Table 1 shows that more than 50.00 % of solar flares of different intensities (except X2.0 - X2.9 intensity level) occurred during the descending phase of the solar cycle 23. Similar results have also been reported by Le et al. (2014) and Bruevich et al. (2017) for solar cycles 21-23. This property is associated with the results reported by Le et al. (2013a) that the descending phase of solar cycles accounts for most of the occurrences of major geomagnetic storms. On average of all flares intensity, 47.00 % and 63.00 % of the flares appeared one year before and two years after (N_{12}) and two years before and three years after (N_{23}) this solar cycle maxima, respectively. But from table 2, we note that during the solar cycle 24 most of the large flares occurred in the ascending phase of the cycle and 76.15 % and 80.80 % of the flares appeared two years before and one year after (N_{21}) and three years before and two years after (N_{32}) these solar cycle maxima respectively. Bruevich et al. (2017) also reported that most of the large flares (≥ X2.7) occurred in the ascending phase and the maximum of solar cycle 24. Table 3 shows that 83.33 % and 75.00 % of the X5.0 - X9.9 flares, were produced by SARs during the 23 and 24 solar cycles respectively, and 100.00 % of ≥ X10 were produced by SARs during the solar cycle 23 and none of ≥ X10 flares occurred in solar cycle 24. This suggests that solar cycle 24 is weaker than 23. Many authors also showed that solar cycle 24 is weaker than 23 (Richardson 2013; Singh et al. 2014; Kakad et al. 2019).

It is supposed that the weak polar fields observed during the solar

activity minimum period of solar cycle 23 are the main cause of the weakness of the solar cycle 24 (Jiang et al. 2015). These weak polar fields were observed due to the results of several bigger bipolar magnetic regions emerging at low latitudes with a `distinct' orientation of their magnetic polarities in the North-South direction, which suppresses the polar field's evolution. Since these magnetic opposite polarities regions emerged within $\pm 10^0$ latitude from the solar equator, they are known to possess a strong effect (Jiang et al., 2015). Le et al. (2013b) reported that in solar cycles 22 and 23, 77.40 % of the ground level enhancements events arise from the Super Active Regions, with 22.60 % from others. Table 3 shows the ratio of different intensity X-class solar flares produced by SARs during cycles 23–24.

IV SUMMARY & CONCLUSIONS

In the present study, statistical distribution corresponding to X-class flares and their inter correlation with super active regions during two recent solar cycles, 23-24 are analyzed and presented. Le et al. (2014) also studied the statistical distributions of X-class flares and their correlation with active regions during solar cycles 21-23 and reported that most X-class flares occurred in the descending phase of the three solar cycles. In the present study, we have selected the next solar cycle 24 along with 23, to observe the trend of distribution of solar flares in different phases of these selected solar cycles. The one basic difference in the present study is that the maxima of solar cycle 23 noted in November 2001 with a maximum of SMSNs is 180.3, whereas in a previous study (Lee et al. 2014) the peak of solar cycle 23 was recorded in April 2000 with maximum sunspot numbers 120.8. Due to this difference the number of flares of different intensities as in table 1, slightly differ in ascending and descending phase of solar cycle 23 in comparison to Lee et al. (2014) work, but the total numbers of solar flares and their distribution trend remain the same.

During the solar cycle, 23-24, a total of 39392 C-class weak solar flares, 3295 M-class moderate solar flares, and 174 X-class intense flares were observed. These X-class intense solar flares are associated with 88 active regions. Out of 88 active regions, only 17 are selected as super active regions. We observe that a more significant number of solar flares occurred in cycle 23 as compared to cycle 24 and more than 50.00 % of flares of different intensities (except X2.0 - X2.9 intensity level) occurred in the descending phase of solar cycle 23, while 60.00 - 65.00 % flares occurred in ascending phase of solar cycle 24. The stronger flares of ≥ X10 occurred only in solar cycle 23. The maximum of SMSNs is 180.3 and 116.4 for solar cycles 23 and 24, respectively. This suggests that solar cycle 24 is weaker than 23. It is also observed that the most intense X-class solar flares occurred during the descending phase of cycle 23. This property is quite similar to that the descending phase of solar cycles accounts for most of the occurrences of gigantic geomagnetic (Le et al. 2013a). Besides, the results correspond that in the solar cycle 24, 50.00 % stronger flares occurred in the ascending phase and 50.00 % in the descending phase of the cycle. Many authors (Ataç et al., 2006; Mariş et al., 2002) also reported that flare activity is low level in the ascending phase and remarkably high in descending phase of solar cycle 23. Bai (2003) reported a high flare activity in the early descending phase of SC 23. It is well known that solar activity on the northern and southern hemispheres of the solar disk is not uniform. In the present study, it is found 58 solar flares occurred in the northern and 67 solar flares occurred in the southern hemisphere of solar cycle 23, It means that solar flare activity dominated in the southern hemisphere for solar cycle 23. During solar cycle 24, 40.80 % (20) solar flares occurred in the northern and 59.10 % (29) flares occurred in the southern hemisphere It is evident that flares of X-class also dominated in the southern hemisphere, but Solar cycle 24 shows the reverse trend in comparison to SC 23, which started in December 2008 and had a double-peaked solar maximum, with the first peak occurring in 2011 and the second peak came in April 2014. Bruevich et al. (2017) have studied the N-S distribution of large (≥ M1) solar flares in solar cycle 24 and reported that strong solar flares dominated in the Northern Hemisphere (NH) in 2011 and shifted to Southern Hemisphere (SH) in 2014. In the present study, the 50.00 % strong flares (of X5.0 - X9.9 level) appeared in NH and 50.00 % in SH (Descending phase).

Joshi and Chandra (2019) have also studied the N-S distribution and asymmetry of GOES SXR flares during solar cycle 24 and reported that more flares occurred in the NH during the ascending phase of the cycle, while during the later phases of the cycle, the excess of flares shifted towards the southern hemisphere. Recently, Isaeva et al. (2020) statistically analyzed the flare activity in solar cycle 24 and reported that 744 flares of M and X-class occurred in solar cycle 24, and out of 744, 310 flares occurred in the northern hemisphere and the remaining 434 occurred in the southern hemisphere. It means that the southern hemisphere was appreciably more active in terms of the number of flares. He also noted that there were 1720 active regions and 234 active regions (13.60 %) were associated with 744 M and X-class. In the present study, we found that 49 X-class solar flares were associated with 29 active regions.

The stronger flares of ≥ X10 occurred only in solar cycle 23. The maximum of SMSNs is 180.3 and 116.4 for solar cycles 23 and 24, respectively. This suggests that solar cycle 24 is weaker than 23. It is also observed that the most intense X-class solar flares occurred during the descending phase of cycle 23. This property is quite similar to that the descending phase of solar cycles accounts for most of the occurrences of gigantic geomagnetic (Le et al. 2013a). Besides, the results correspond that in the solar cycle 24, 50.00 % stronger flares occurred in the ascending phase and 50.00 % in the descending phase of the cycle. Mohamed et al. (2018) also showed that most power full solar flares occurred in descending phase of the solar cycle 23.

From Tables 1 and 2, it can also see that 100.00 % of the X3.0

- X4.9 flares appeared in the vicinity of maxima of solar cycle 24, whereas only 50.00 - 60.00 % of this level flares occurred around the solar maxima of solar cycle 23. Table 3 shows that SARs in cycle 23 produced 83.33 % of ≥X5 and 100.00 % of ≥ X10 flares. 75.00 % of ≥X5 were produced by SARs and none of ≥ X10 flares in solar cycle 24. Table 4 shows the properties of selected SARs during solar cycles 23-24.

From the above results and discussion, we can conclude that there were total 174 X-class flares generated by 88 active regions during solar cycles 23-24. Of the 58.62 % at X1.0 - X1.9 intensity level, 17.24 % at X2.0 - X2.9 intensity level, 11.49 % at X3.0 - X4.9 intensity level, 9.19 % at X5.0 - X9.9 intensity level and 3.44 % at ≥ X10 level.

Solar flare activity is low in ascending phase and high in descending phase of solar cycle 23 (due to excess of more flares activity in SH).

Solar flare activity is high in ascending phase (due to excess of high flare activity in NH in 2011) and low in descending phase of solar cycle 24 (Negative result, because flare activity high in SH in 2014).

Super Active Regions (SARs) produced 27.77 % of X1.0 - X1.9, 36.84 % of X2.0 - X2.9, 43.75 % of X3.0 - X4.9, 83.00 % of X5.0 - X9.9, and 100.00 % of ≥ X10 level in solar cycle 23.

During solar cycle 24, 20.00 % of X1.0-X1.9, 36.36 % of X2.0 - X2.9, 25.00 % of X3.0 - X4.9, 75.00 % of X5.0 - X9.9, and none of ≥ X10 level were produced by Solar Active Regions.

Statistical distribution of flares and maximum monthly sunspots numbers during solar cycles 23-24 show that solar cycle 24 is substantially weaker than solar cycle 23.

Strong solar flares ≥ X10 levels are associated with super active regions produced by a stronger solar cycle. For example, strong flares X28.0, X17.2, and X10.0 are associated with super active region 10486, and X20.0, X17.0, and X14.4 are produced from 9393, 10808, and 9415 SARs respectively, during solar cycle 23.

It is also noted that most strong flares associated SAR (10486) have a maximum flare index (77.74) in comparison to other listed SARs in table 4.

Note: Table 1, 2, 3 & 4 has been shown in appendix.

ACKNOWLEDGMENT

It The work is supported by SERB, New Delhi, for the CRG project (File No: CRG/2019/000573). Authors are thankful to the sunspot index and long-term solar observation (SILSO) world data center for SMSNs data from the webpage: http://www.sidc.be/silso/datafiles#total. Authors are also thankful to NOAA/NASA for providing the X-ray solar fluxes by satellite GOES-15 from the website: https://www.spaceweatherlive.com/en/archive.

REFERENCES

Ataç T, Özgüç A, Rybak J 2006 Periodicities in irradiance and in other solar activity indices during Cycle 23; Solar Phys. 237, 433-444.

Bai T 1988 Distribution of flares on the Sun during 1955-1985 - "Hot spots" (active zones) lasting for 30 years; Astrophys. J. 328, 860. https://doi.org/10.1086/166344

Bai T 1987 Distribution of flares on the Sun - Superactive regions and active zones of 1980-1985; Astrophys. J. 314, 795. https://doi.org/10.1086/165105

Bai T 2003 Periodicities in solar flare occurrence: analysis of cycles 19–23; Astrophys. J. 591, 406-415.

Bruevich E A, Kazachevskaya T V, Yakunina G V 2017 Large Flares (M1–X7) in Solar Activity Cycle 24; Geomagn. Aeron. 57, 1077–1085. https://doi.org/10.1134/S0016793217080059

Bruzek A 1972 Properties of Solar Active Regions, in de Jager, C, Dyer ER (Eds.), Astrophysics and Space Science Library. Springer Netherlands, Dordrecht, pp. 49–60. https://doi.org/10.1007/978-94-010-3126-4_5

Carrington R C 1859 Description of a Singular Appearance seen in the Sun on September 1, 1859; Mon. Not. R. Astron. Soc. 20, 13–15. https://doi.org/10.1093/mnras/20.1.13

Chen A, Wang J 2015 Super-active regions in solar cycle 24; Proc. Int. Astron. Union 11, 309–314. https://doi.org/10.1017/s1743921316000223

Chen A Q, Wang JX, Li JW, Feynman J, Zhang J 2011 Statistical properties of superactive regions during solar cycles 19–23; Astron. Astrophys. 534, A47. https://doi.org/10.1051/0004-6361/201116790

Harra L K, Schrijver C J, Janvier M, Toriumi S, Hudson H, Matthews S, Woods M M, Hara H, Guedel M, Kowalski A, Osten R, Kusano K, Lueftinger T 2016 The Characteristics of Solar X-Class Flares and CMEs: A Paradigm for Stellar Superflares and Eruptions? Sol. Phys. https://doi.org/10.1007/s11207-016-0923-0

Isaeva ES, Tomozov VM, Yazev SA 2020 X-Ray Flares and Activity Complexes on the Sun in Solar Cycle 24; Astron. Reports 64, 58–65. https://doi.org/10.1134/S1063772920010035

Jiang J, Cameron R H, Schüssler M 2015 The cause of the weak solar cycle 24; Astrophys. J. 808, L28. https://doi.org/10.1088/2041-8205/808/1/L28

Joshi A and Chandra R 2019 North-South Distribution and Asymmetry of GOESSXR Flares during Solar Cycle 24; Open Astron. 28, 228-235.

Kakad B, Kakad A, Ramesh DS, Lakhina G S 2019 Diminishing activity of recent solar cycles (22–24) and their impact on geospace;J. Space Weather Space Clim. 9,15.https://doi.org/10.1051/swsc/2018048.

Le G M, Cai ZY, Wang H N, Yin ZQ, Li P 2013a Solar cycle distribution of major geomagnetic storms; Res. Astron.

Astrophys. 13, 739–748. https://doi.org/10.1088/1674-4527/13/6/013

Le G M, Li P, Yang H G, Chen YL, Yang XX, Yin ZQ 2013b The properties of solar active regions responsible for ground-level enhancements during solar cycles 22 and 23; Res. Astron. Astrophys. 13, 1219–1224. https://doi.org/10.1088/1674-4527/13/10/009

Le G, Yang X, Liu Y, Li P, Yin Z, Chen Y 2014 Statistical properties of X-class flares and their relationship with super active regions during solar cycles 21–23; Astrophys. Space Sci. 350, 443–447. https://doi.org/10.1007/s10509-013-1773-y

Li W, Wang H 1997 An analysis on the strongest active regions of solar cycle 21; Publ. Yunnan Obs. 1, 10–17.

Mariş G, Popescu, M D, Mierla M 2002 The North-South Asymmetry of Soft X-Ray Solar Flares; Romanian Astro. J. 12, 131-146.

Mohamed W, Yousef S, Shaltout M 2018 On the classifications of the solar active regions (ARs); Case study for solar cycles 23 and 24; Egypt. J. Remote Sens. Sp. Sci. 21, 249–253. https://doi.org/10.1016/j.ejrs.2017.04.004

Richardson I G 2013 Geomagnetic activity during the rising phase of solar cycle 24; J. Space Weather Space Clim.3, 11.https://doi.org/10.1051/swsc/2013031

Romano P, Zuccarello F 2007 Photospheric magnetic evolution of super active regions; Astron. Astrophys. 474, 633–637. https://doi.org/10.1051/0004-6361:20078110

Roy J R 1977 The north-south distribution of major solar flare events, sunspot magnetic classes and sunspot areas (1955–1974); Sol. Phys. 52, 53–61. https://doi.org/10.1007/bf00935789

Sammis I, Tang F, Zirin H 2000 The Dependence of Large Flare Occurrence on the Magnetic Structure of Sunspots; Astrophys. J. 540, 583–587. https://doi.org/10.1086/309303

Schwabe H, Schwabe H 1844 Sonnen — Beobachtungen im Jahre 1843; Astron. Nachrichten 21, 234–235. https://doi.org/10.1002/asna.18440211505

Singh A K, Tonk A 2014 Solar activity during first six years of solar cycle 24 and 23: a comparative study; J. Astrophysics and Space Phys.353, 367-373. DOI: 10.1007/s10509-014-2067-8

Tian L, Liu Y. Wang J 2002 The most violent super-active regions in the 22nd and 23rd cycles; Sol. Phys. 209, 361–374. https://doi.org/10.1023/a:1021270202680

van Driel-Gesztelyi L, Green L M 2015 Evolution of active regions; Living Rev. Sol. Phys. 12, 1–98. https://doi.org/10.1007/lrsp-2015-1

Wang H, Liu C 2015 Structure and evolution of magnetic fields associated with solar eruptions; Res. Astron. Astrophys. https://doi.org/10.1088/1674-4527/15/2/001

Wu M, Zhang Q 1995 The strongest active regions for solar cycle 22; Publ. Yunnan Obs. 1, 1–12.

Yang YH, Hsieh M S, Yu H S, Che, P F 2017 A statistical study of flare productivity associated with sunspot properties in different magnetic types of active regions; Astrophys. J. 834, 150. https://doi.org/10.3847/1538-4357/834/2/150

APPENDIX

Table 1: The statistical distributions of all X –class flares in solar cycle 23.

Flare intensity	N_a	N_d	N_t	Ratio N_a/N_t	Ratio N_d/N_t	N_{12}	N_{23}	Ratio N_{12}/N_t	Ratio N_{23}/N_t
X1.0-X1.9	33	39	72	45.83%	54.16%	32	52	44.00%	72.20%
X2.0-X2.9-	12	7	19	63.15%	36.84%	8	11	42.00%	58.00%
X3.0-X4.9	5	11	16	31.25%	68.75%	8	9	50.00%	56.25%
X1.0-X4.9	50	57	107	46.72%	53.27%	48	72	45.00%	67.20%
≥X5	6	12	18	33.33%	66.67%	10	11	55.50%	61.10%

Note: N_a and N_d denote flare numbers in the ascending and descending phases of solar cycle 23, respectively. $N_t$denotes the total number of solar flares that occurred during a solar cycle. N_{12} represents the number of solar flares that occurred one year before the solar cycle peak and the two years after it. N_{23} represents the number of solar flares that occurred two years before the solar cycle peak and the three years after it. To see more distribution of flares around the peak, asymmetry time windows are considered, because before the peak (in ascending phase) the number of flares is lesser than after peak (in descending phase).

Table 2: The statistical distributions of all X –class flares that occurred in solar cycle 24.

Flare intensity	N_a	N_d	N_t	Ratio N_a/N_t	Ratio N_d/N_t	N_{21}	N_{32}	Ratio N_{21}/N_t	Ratio N_{32}/N_t
X1.0-X1.9	21	9	30	70.00%	30.00%	21	28	70.00%	93.00%
X2.0-X2.9-	5	6	11	45.50%	54.54%	7	8	63.60%	72.70%
X3.0-X4.9	3	1	4	75.00%	25.00%	4	4	100.00%	100.00%
X1.0-X4.9	29	16	45	64.44%	35.55%	32	40	71.10%	88.88%
≥X5	2	2	4	50.00%	50.00%	nil	nil		

Note: N_a and N_d denote flare numbers in the ascending and descending phases of solar cycle 24, respectively. N_t denotes the total number of solar flares that occurred during this solar cycle. N_{21} represents the number of solar flares that occurred two years before the solar cycle peak and one year after it. N_{32} represents the number of solar flares that occurred three years before the solar cycle peak and the two years after it, because before the peak (in ascending phase) the number of flares is higher than after peak (in descending phase)

Table 3: The ratio of different intensity X-class flares produced by SARs during solar cycles23-24.

Cycle No.	**ARs**	**SARs**	$\mathbf{N_{1SAR}/N_{1t}}$	$\mathbf{N_{2SAR}/N_{2t}}$	$\mathbf{N_{(3\text{-}4)\,SAR}/N_{(3\text{-}4)\,t}}$	$\mathbf{N \geq_{5\text{-}9.9\,SAR}/N_t}$	$\mathbf{N_{10SAR}/N_t}$
Solar cycle 23	59	12	21/72= 29.16%	7/19= 36.84%	7/16= 43.75%	10/12= 83.33%	6/6= 100.00%
Solar cycle 24	29	5	6/30= 20.00%	4/11= 36.36 %	1/4= 25.00%	3/4= 75.00%	0.00%

Note: N_{1t} and N_{1SAR} denote the total numbers of X1.0-X1.9 and the numbers of X1.0-X1.9 solar flares produced by SARs during solar cycles 23 and 24 respectively. N_{2t} and N_{2SAR} indicate the total numbers of X2.0-X2.9 and the numbers of X2.0-X2.9 solar flares produced by SARs during solar cycles 23 and 24 respectively.$N_{(3\text{-}4)t}$ and $N_{(3\text{-}4)SAR}$ represent the total numbers of X3.0-X4.9 and the numbers of X3.0-X4.9 solar flares produced by SARs during solar cycles 23 and 24 respectively. Remains can be understood in the same manner.

Table 4: List of super active regions and their properties during solar cycles 23-24.

	SARs Region	Date and Location of sunspot start	Date and Location of sunspot end	Max SSN	Max. Area (μh)	Flare index	10.7 cm flux *(s. f. u.)*	days of β-γ-δ magnetic field of sunspot group	Number of flares observed during SARs	Northern/ Southern Hemisphere
Solar Cycle 23	8100	28/10 /1997 S21E67	08/11/1997 S19W77	37	1000	12.28	3400	3	C=24 M=4 X=2	S
	8307	20/08/1998 N32E72	02/09/1998 N32W90	18	570	15.75	2720	Nil	C=11 M=5 X=5	N
	9077	08/07/2000 N18E72	21/07/2000 N19W84	62	1010	11.68	3700	6	C=15 M=12 X=3	N
	9393	24/03/2001 N20E65	04/04/2001 N18W94	63	2440	27.84	11000	9	C=28 M=4 X=2	N
	9415	04/04/2001 S22E72	16/04/2001 S21W87	40	880	27.42	48000	6	C=16 M=6 X=5	S
	10069	12/08/2002 S08E77	24/08/2002 S08W85	74	1990	8.51	1600	11	C=55 M=17 X=2	S
	10484	19/10/2003 N05E68	31/10/2003 N01W95	69	1750	6.01	2500	10	C=30 M=16 X=2	N
	10486	23/10/2003 S16E81	05/11/2003 S17W89	108	2610	77.56	20000	13	C=19 M=16 X=7	S
	10488	28/10/2003 N09E09	05/11/2003 N08W95	61	1750	7.78	6100	7	C=17 M=7 X=2	N
	10720	11/01/2005 N09E65	23/01/2005 N11W93	54	1630	21.06	12000	3	C=66 M=17 X=5	N
	10808	08/09/2005 S12E83	20/09/2005 S11W78	80	1430	46.92	27000	8	C=47 M=20 X=10	S
	10930	06/12/2006 S06E72	18/12/2006 S06W88	18	680	21.84	65000	10	C=45 M=5 X=4	S

Solar Cycle 24	11429	04/03/2012 N18E68	16/03/2012 N19W85	28	1270	11.87	12000	7	C=32 M=14 X=2	N
	11520	08/07/2012 S15E54	19/7/2012 S17W89	60	1460	2.92	1000	7	C=26 M=6 X=1	S
	11944	02/01/2014 S07E75	16/01/2014 SS12W0	118	1560	2.68	8300	9	C=44 M=8 X=1	S
	12192	18/10/2014 S13E68	01/11/2014 S15W0	66	2750	19.59	580	11	C=66 M=31 X=6	S
	12673	30/08/2017 S08E62	10/09/2017 S09W83	33	1000	28.11	185.5	7	C=45 M=27 X=4	S

Note: Flare index is calculated by summation of intensities of M-class flares multiplied by 0.1 and X –class flares multiplied by 1 associated with SARs

***